Journal of South American Earth Sciences 58 (2015) 141–147

Contents lists available at ScienceDirect

Journal of South American Earth Sciences

journal homepage: www.elsevier.com/locate/jsames

New evidences of rupture of crust and mantle in the subducted Nazca plate at intermediate-depth

Silvana L. Spagnotto [a, b, *], Enrique G. Triep [c], Laura B. Giambiagi [d], Silvina V. Nacif [a, c], Orlando Álvarez [a, c]

[a] CONICET, Argentina
[b] Departamento de Física, Universidad Nacional de San Luis, Ejército de los Andes 950, 5700, San Luis, Argentina
[c] IGSV, Universidad Nacional de San Juan, Ruta 12, Km 17, San Juan, Argentina
[d] IANIGLIA-CCT Mendoza-CONICET, Argentina

ARTICLE INFO

Article history:
Received 4 July 2014
Accepted 17 December 2014
Available online 31 December 2014

Keywords:
Coulomb static stress
Intermediate-depth seismicity
Subducted Nazca plate
Outer-rise faults

ABSTRACT

Between 33°–36°S, the Nazca plate subducts below South American plate with an angle of ~30°, and it is seismically active until ~200–280 km depth. At 33.5°S, the seismicity decreases drastically at 120 km depth, just below the volcanic arc. In this paper, we studied a pair of associated earthquakes located in the area where the frequency of seismicity changes. The hypocenters of the $M_w = 6.4$, June 16th, 2000 and $M_w = 5.7$ January 7th, 2003 earthquakes were found nearby, adjacent to the oceanic Moho, closely associated with each other. The slip on the plane of the 2000 event produced Coulomb stress changes on the fault plane of 2003, both westward dipping, with a variation from ~1 bar near the hypocenter of the latter to ~0.1 bars in the deepest part of the plane. The two earthquakes combined process describes a normal focal mechanism, which cuts through the crust and breaks the mantle, reaching depths of ~40 km below the Moho.

The composed fault plane of the 2000 and 2003 events corresponds to a west-dipping normal fault with strike and dip consistent with those of the outer ridge faults. Thus, these events could be related to a preexisting fault originated in that environment reactivated at depth.

The slip on the composed fault plane is consistent with the bending produced by the slab pull. Dehydration could be associated to these events.

1. Introduction

The studied earthquakes are placed along the northern segment of normal subduction of the Nazca plate below the South American plate, at approximate 33.5°S latitude. In this area, there is a noticeable decreasing of the Nazca intraplate seismicity below 120 km depth (Fig. 1a and b). To the north of this segment, the Nazca plate flattens at 100 km depth and continuous visible below the South American plate by registered seismicity (Anderson et al., 2007). Southward of 34.5°S seismicity continues without a sharp decline (Spagnotto, 2013; Anderson et al., 2007). Considering the lack of seismicity below 120 km depth, the goal of this work is to understand the seismicity behavior located just where this change occurs. Two quakes situated at that point were processed and analyzed to advance in this issue (at 33.8°S).

The $M_w = 6.4$, June 16th, 2000 and $M_w = 5.7$ January 7th, 2003 intermediate earthquakes, located at 33.895°S, 70.344°W and 33.775°S, 70.304°W respectively were analyzed (Fig. 1a). We found that these earthquakes are closely related to each other with both hypocenters located near the oceanic Moho (Fig. 1b). The former breaks the oceanic subducted crust, increasing the Coulomb static stress around ~1 bar in the area where the rupture of the latter began. The rupture of the second event was entirely developed in the oceanic mantle, cutting up to 40 km in depth.

We calculated mechanisms and depths from waveform inversion and obtained the slip distribution using direct modeling. In the second procedure a new depth, magnitude and focal mechanism according to the lower RMS (Root Mean Square) adjustment of all waveforms, were obtained.

For the 2003 earthquake, the fault plane was defined by aftershocks (Figs. 2 and 3), previously determined by Marot et al. (2012);

* Corresponding author. Departamento de Física, Universidad Nacional de San Luis, Ejército de los Andes 950, 5700, San Luis, Argentina.
E-mail address: pampa113@gmail.com (S.L. Spagnotto).

http://dx.doi.org/10.1016/j.jsames.2014.12.002
0895-9811/

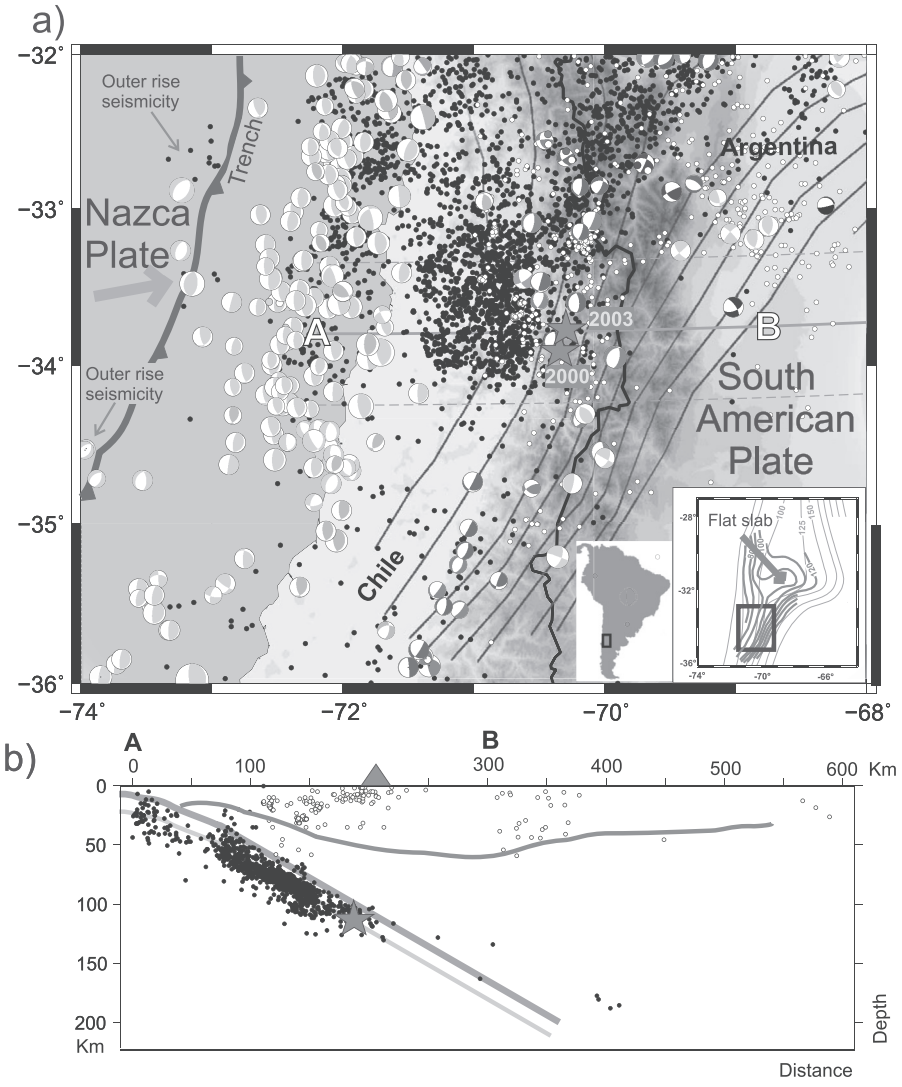

Fig. 1. Regional seismicity. a) Plan view. EHB catalog seismicity: black and White circles correspond to Nazca and South American plate events, respectively. Big black dots are the 2000 and 2003 earthquakes analyzed here. Focal mechanisms are from CMT catalog. These are shown by lower hemisphere projections with dark colors indicating compressional quadrants. Straight dash lines limit the proyected area for AB cross-section (straight black line). The small rectangle at the lower right corner shows the Nazca plate morphology by Cahill and Isacks (1992) – light lines- and Anderson et al. (2007) – dark lines. b) AB Cross-section: EHB catalog seismicity: black and White circles correspond to Nazca and South American plate events, respectively. Star is the place where the 2000 and 2003 earthquakes occur. Lines show continental and oceanic Moho and upper limit of subducted Nazca plate.

while for the 2000 earthquake, we defined the fault plane by association with the 2003 earthquake.

2. Tectonic environment

The Nazca plate is subducted beneath the South American plate at a rate of 6.7 ± 0.2 cm/yr, with a N78° E direction, as constrained by GPS measurements along the Chile–Peru oceanic trench (Kendrick et al., 2003). The subduction area is seismically and tectonically characterized by along-strike variations in slab dip angle (Barazangi and Isacks, 1976; Jordan et al., 1983; Cahill and Isacks, 1992). In the segment between 28° and 32°S, the subduction angle is subhorizontal, while to the south of these latitudes the angle of subduction is ~27° (Cahill and Isacks, 1992; Anderson et al., 2007). The earthquakes studied are placed along the transitional zone between subhorizontal and normal subduction segments (Fig. 1a).

Seismicity associated with subduction of oceanic plates can be classified accordingly to the affected area into: outer rise, underthrusting, intermediate, and deep zones (Kearey et al., 2009). The outer rise earthquakes are related to normal faults generated by the oceanic plate bending mainly (Fig. 1b). Along these faults, fluids could penetrate into the mantle up to at least 7 km (Fisher, 1996; Grevemeyer et al., 2005; Contreras-Reyes et al., 2007; Contreras-Reyes and Osses, 2010), and even deeper up to 30 km, as suggested by stress maps carried out by Faccenda et al. (2009). The underthrusting zone corresponds to the interplate seismogenic zone, where the biggest earthquakes are produced by movement along the mega thrust fault (Fisher, 1996). The intermediate earthquakes in a subduction environment have been related to slab pull forces and dehydration processes of the slab (Kirby et al., 1996; Meade and Jeanloz, 1991; Hacker et al., 2003; Jung et al., 2004; Jung et al. 2009). Jiao et al. (2000) and Ranero et al. (2003) propose the reactivation of preexisting normal faults of the slab at intermediate depths.

Ranero et al. (2005), analyzing the oceanic bathimetry, classified the preexisting faults in the Nazca plate along the Chilean coast. Three mechanisms that produce normal fault populations are

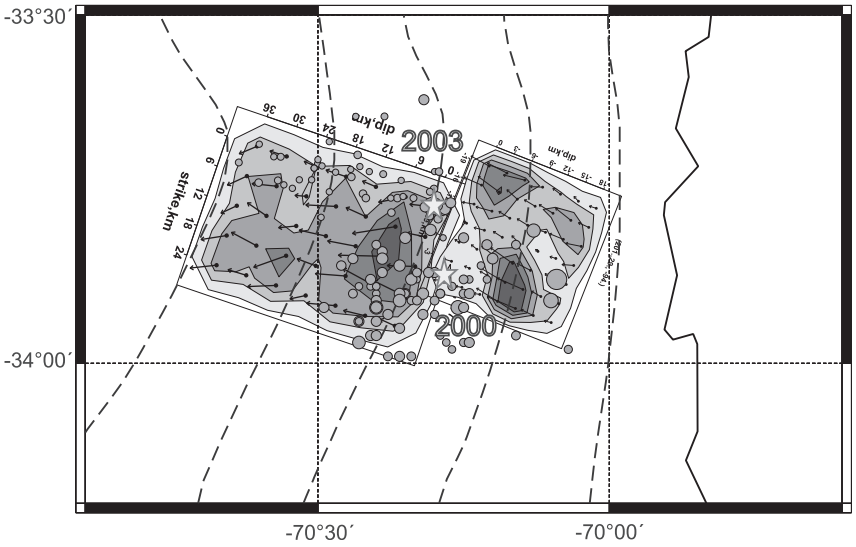

Fig. 2. Slip distributions for the 2000/06/16 and 2003/01/07 quakes. Strike/dip/rake are 201/29/-91 and 199/38/-79 respectively. In light gray 2003 aftershocks and in gray 2000 aftershocks. Dash lines are morphology of the subducted plate obtained from Nacif (2012).

documented: (i) faults related to seafloor spreading fabric, striking ~145° for the latitudes of this study; (ii) bending faults subparallel to the trench; and (iii) faults parallel to the Juan Fernández ridge, striking ~60°. During subduction, conjugated normal faults of these three populations, dipping ~60° both to the east and west, suffer a clockwise ~30° rotation along a horizontal N-trending axis, becoming subvertical and subhorizontal at depth respectively (Fig. 1b). Warren et al. (2008) document that from 40 to 100 km depth, earthquake ruptures can exist along both subhorizontal and subvertical faults. However, deeper than 100 km depth, reactivated planes are preferably subhorizontal (Warren et al., 2008).

3. Methodology

Focal mechanisms and slip distributions with Teleseismic Body-Wave Inversion Program (Kikuchi and Kanamori, 1991, 1982; Kikuchi et al., 1993) were obtained. Kikuchi–Kanamori method uses P-waves and S-waves from teleseismic distances between ~20° and 90°. This software describes the seismic source as a sequence of point sources with one or various focal mechanisms (Kikuchi and Kanamori, 1991). The point sources are determined iteratively by matching between observed records and synthetic ones. The software uses a moment tensor to describe each point

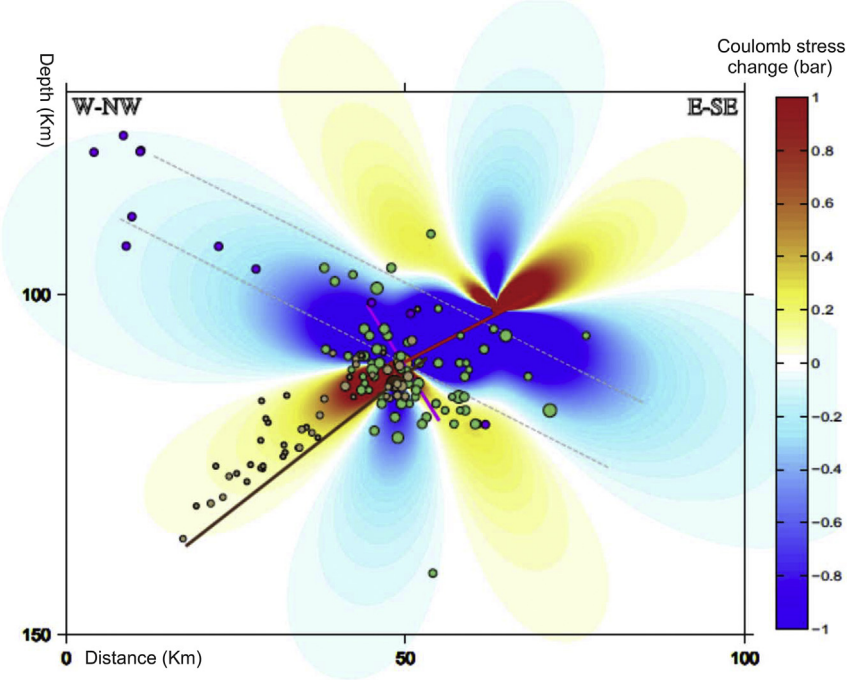

Fig. 3. Cross-section showing spatial organization of the 2000/06/16 and 2003/01/07 earthquakes, its aftershocks, and ruptures. In brown, 2003 aftershocks, and in green 2000 aftershocks. In violet earthquakes obtained from Nacif (2012). Calculation of Coulomb stress change using earthquake source 2000 with strike 201, dip 29 and rake −91 and receptor fault 199/38/-79 (2003 quake). (For interpretation of the references to color in this figure legend, the reader is referred to the web version of this article.)

source. It is based in linear combination of six elementary moment tensor. The advantage of this system is that allow to obtain moment tensor generally, deviatric or double couple (using all elementary moment tensor or some of them). In the inversion, the hypocenter (latitude, longitude, depth and origin time), rupture velocity and source duration are fixed. The time arrival in the stations is calculated using Jeffreys and Bullen velocity tables. The software permits to put a shift if the arrival is offset (Kikuchi and Kanamori, 2003).

To calculate the Green's functions, the software uses a velocity model for the region of the earthquake and another for the stations. The Green function is calculated for an initial depth. To obtain the depth that best fits, we repeated the inversion with different initial value. The same proceeding were made for other fix parameters such rupture velocity and temporal function (Kikuchi and Kanamori, 2003).

Slip distribution Kikuchi–Kanamori software is based on method of Hartzell and Heaton, 1983. This takes a rectangular plane, representing the fault plane, for fixed values of strike, dip, and dimension. This plane is gridded, and the amount of slip and the time history of slip at each grid point are determined. Since the fault plane and the rupture front speed are fixed, the inversion remains stable. The rake angle is constrained between ±45° of the prescribed rake angle. A smoothness constraint can also be imposed and maximum rupture velocity is fixed. In every seismic station, the response of each point source is calculated as the sum of all cell, whit their respective delays (Kikuchi and Kanamori, 2003). The initial fault plane in slip distributions was obtained from inversion and the CMT solutions of 2000 and 2003 earthquakes, and then the best fit of the two solutions in each case was chosen. We resolved slip distributions in both fault planes.

We performed point-source inversions using broadband body waveforms (vertical P and transverse S) downloaded from IRIS Data Management Center (USA). The stations used in each case are indicated in Figs. 4 and 5. The localizations used as input for these inversions are: (1) For the 2003 earthquake, the one obtained by Marot et al. (2012), and (2) for the 2000 earthquake, we chose the most consistent results for the localization. For (2) the value is −33.895°S, −70.344°W, 112 km. This is the PDE epicenter shifted towards W–SW equally to the 2003 earthquake changes in the localization obtained by Marot et al. (2012) respect to the PDE catalog.

We used between 80 and 100 s for the time of records with high-pass filter: 0.002 Hz and low-pass filter: 0.1 Hz in the inversions. In slip distributions we used 80–120 s and low-pass filter 0.4 in the first earthquake (Fig. 4) and 0.25 in the second (Fig. 5). We converted to ground displacement with a sampling time of 0.5 s.

We used Jeffreys and Bullen (1958) velocity model for each receptor station, and Nacif (2012) velocity model for near-source structure. Table 1 shows the focal mechanisms, depths, rupture area, stress drop, maximum slip, rupture velocity, and temporal function obtained.

During the implementation of the inverse method, we evaluate the RMS at depths between 100 and 150 km and chose the lowest value. This allows us to obtain reliable depth values. For the 2000 earthquake, the initial depth of 128 km was modified to 110 km with the inverse modeling, and to 110–115 with the forward modeling performed to obtain the slip distribution. For the 2003 quake, the initial depth of 113 km was reduced to 108 km with the inverse method, and 113 km with the forward modeling.

The time function used in the inverse method was modified in order to obtain a minimum RMS. In all cases, the shape of the temporal function that best fits the results is a triangular function. Source durations were 13 s and 15 s for the 2000 and 2003 events respectively. These results are considered a bit high for earthquakes of magnitude $M_w = 5.7$ and $M_w = 6.4$ respectively, if they were located on the upper crust. However, Frolich (2006) shows that the source duration *versus* the seismic moment for earthquakes deeper than 100 km has slightly longer time periods.

Moreover, the inverse method allows the maximum rupture velocity to be obtained. In the study case, the 2000 and 2003 earthquakes yielded rates of 1.9–2.0 km/s and 2.9 km/s, respectively. Both of these values are consistent with the results of Xia et al. (2004). These authors use mimic earthquakes to estimate the velocity of rupture V_r of the S wave velocity between 0.3 and 0.9.

Coulomb static stress changes were calculated using Coulomb 3.2 software (Toda et al., 2005; Lin and Stein, 2004).

4. Results

Width and length of slip distributions for the 2000 and 2003 events, obtained by forward modeling, imply anomalously large

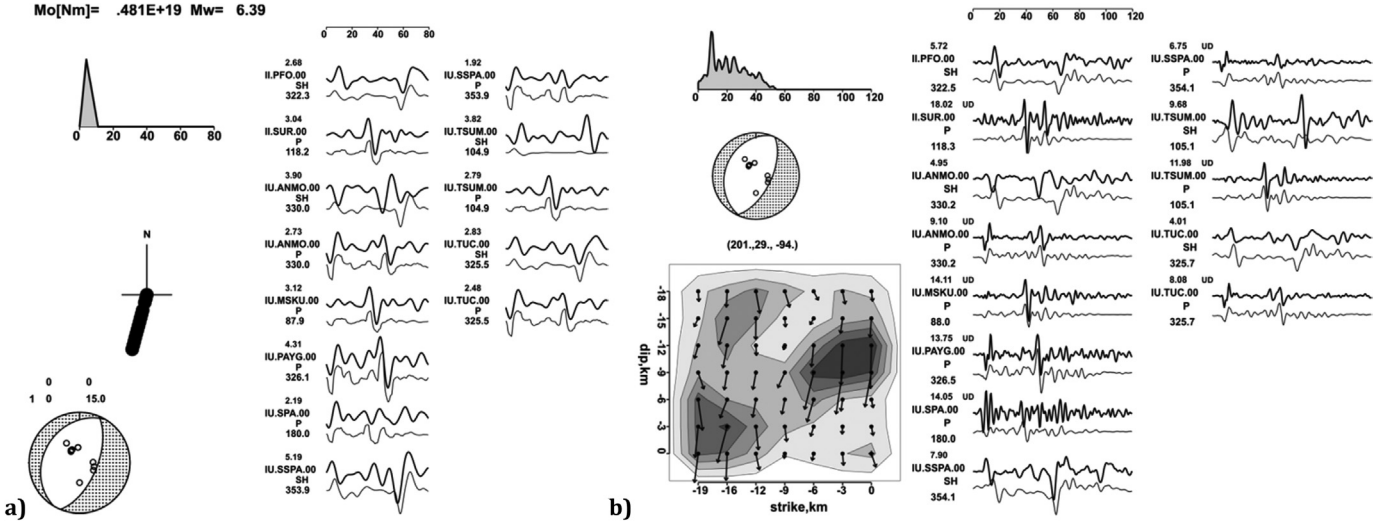

Fig. 4. a) Inversion for the 2000/06/16 earthquake using Kikuchi and Kanamori Software. High-pass filter: 0.002 Hz. Low-pass filter: 0.1 Hz. RMS 0.4443. b) Slip distribution. High-pass filter: 0.002 Hz low-pass filter: 0.4 Hz. RMS 0.4189.

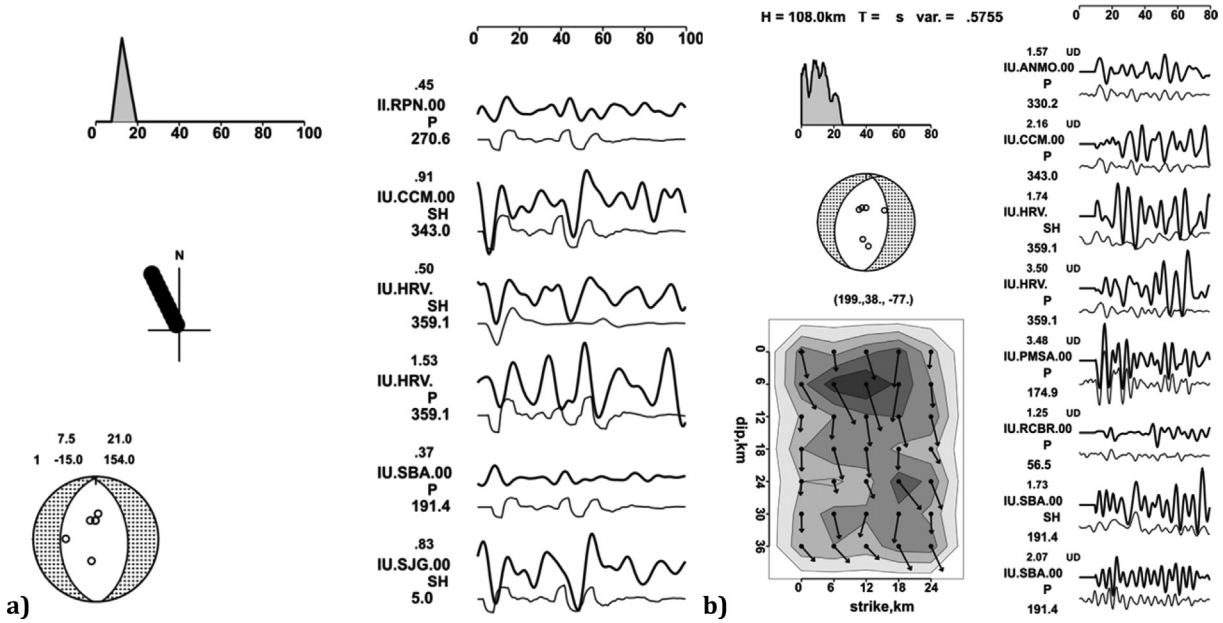

Fig. 5. a) Inversion for the 2003/01/07 earthquake using Kikuchi and Kanamori Software. High-pass filter: 0.002 Hz low-pass filter: 0.01 Hz. RMS 0.7649. b) Slip distribution. High-pass filter: 0.002 Hz low-pass filter: 0.25 Hz. RMS 0.5755.

areas of 342 and 864 km^2. This also occurs for the area estimated by Marot et al. (2012) of the 2003 event, which varies from 240 to 400 km^2. These values are larger than the 60 km^2 calculated by Wells and Coppersmith (1994) for crustal earthquakes. This suggests a different rheological rupture behavior for these intermediate-deep earthquakes when compared to crustal earthquakes.

To calculate the static stress drop, we used $\Delta\sigma = cMo/LA$, where Mo is scalar moment, L, fault length, A, area obtained from slip distributions and c, constant ($c = 3.5$) that considers the fault geometry (Frolich, 2006).

Frolich (2006) compiled and compared studies from various authors, and showed that the static stress drops vary from 50 to 1000 bar for intermediate and deep earthquakes of magnitude $M_w > 6.3$. The differences between the values depend mainly on fault dimensions. Static stress drops up to 200 bars are reported for earthquakes of magnitudes lower than 6. For the 2000 crustal earthquake, 48 bars are closed to these values, but 0.2 bars for the 2003 mantle earthquake, suggests a different rupture behavior.

The software calculates area and maximum slip (Table 1) depending on an assumed rigidity value. We used 65×10^9 Pa corresponding to the mantle at 100 km depth (Masters et al., 1995). Waveform inversion allows us obtaining the general moment tensor, specifying isotropic and CLVD (Compensated Linear Vector Dipole) components. The most commonly reported percentage of isotropic component for intermediate deep earthquakes is about ~10% or less but it is never equal to zero (Kawakatsu, 1991, 1996). The 2000 earthquake presents 6% of CLVD and 15% of isotropic component and the 2003 earthquake presents a 3% of CLVD and 13% of isotropic component. Kubas and Sipkin (1987) analyzed the CLVD components in earthquakes of subducted Nazca plate, reaching a minimum value of 6% and a maximum value of 16%. Particularly, Kubas and Sipkin (1987) studied the 15th December 1983 earthquake which is located very close to the 2000 and 2003 quakes and it has a value of 1% de CLVD. These low values of isotropic and CLVD percentages suggest that during these seismic events there is little volumetric changes and the faults behave predominantly as double-couple.

5. Discussion

For the $M_w = 5.7$, 7th January 2003 earthquake, Marot et al. (2012), studying the distribution of aftershocks, suggested that the activated fault plane dips to the west. Therefore, to obtain the slip distribution on this plane we chose the nodal plane dipping west from the three following focal mechanism: (1) the one obtained in our inversion, (2) the one got through CMT catalog and (3) the one proposed by Marot et al. (2012). The slip distribution that best fits the aftershocks is the one obtained using the CMT mechanism, which prompts us to select it as the best solution for the

Table 1
Focal mechanisms for the 2000 and 2003 earthquakes from CMT catalog, and obtained with inversion and slip distributions. Rupture areas and velocity, static stress drops, maximum slip, and temporal function obtained in this work.

Date	Focal mechanism (strike/dip/rake Aki and Richards, 1980 convention)						Rupture area (km^2)	Static stress drop (bar)	Maximum slip (m)	Rupture velocity (km/s)	Temporal function (s)
	CMT source		Inversion solution		Solution with minimum RMS in slip distribution						
2000/06/16	219/33/-67 11/60/-105 Mw = 6.4	Depth 109 km	201/29/-88 19/61/-91 Mw = 6.38	Depth 110	201/29/-91 15/58/-86	Depth 105 km	342	48	0.75	1.9 to 2	13
2003/01/07	199/28/-70 356/64/-100 Mw = 5.7	Depth 113 km	182/43/-85 355/47/-94 Mw = 5.98	Depth 108 km	199/38/-79 With CMT Solution	Depth 108 km	864	0.2	0.1	2.9	15

earthquake (Fig. 2). In the slip distribution, the largest release of energy is concentrated in two areas along the fault plane. The determined aftershocks are located in one of these zones (Fig. 2). The slip distribution from the mechanism obtained by Marot et al. (2012) is not consistent with the aftershocks.

The increased stress produced by the 2000 earthquake (Fig. 3) explains the aftershock activation of the 2003 earthquake, reaching values of 1 bar near the epicenter, declining to 0.1 bars in the deepest part of the fault plane. The eastward dipping nodal plane of the earthquake focal mechanism only generates less than 0.1 bar stress variations in a small area of aftershocks; hence it cannot explain the 2003 earthquake activation.

The fault plane area in the first event with $M_w = 6.4$ (21×24 km^2) accounts for only ~58% of the second event area with $M_w = 5.7$ (24×36 km^2), which might imply that at intermediate depths the rheological conditions for the rupture in the oceanic mantle might be significantly different of those in the corresponding subducted crust.

The aftershocks of the two events are mainly related to areas of moderate to small slip on the activated fault planes, since they are located among areas of maximum slip (Fig. 2). The 2000 rupture develops from the bottom to the top through the entire crust, while the 2003 rupture develops inversely across in the mantle.

In the 2000 reactivated fault plane, the L/W > 1 ratio (L = length of the fault plane along the strike, W = fault plane width along dip), while for the 2003 reactivated plane, L/W < 1 (~0.7). Crustal continental earthquakes, present L/W ratios of $L \approx 1$ or $L > 1$. This difference can be explained by a rheological discontinuity at depth that would stop the downward rupture (Scholz, 1994; Triep and Sykes, 1997). In this sense, the 2003 event in the oceanic subducted mantle behaves as a rheological unbounded earthquake.

We propose that both earthquakes are related since: i) their hypocenters, at 108 km and 110 km depth (Table 1), are close to the Moho and nearly underneath the 100 km contour line (Fig. 2). ii) the strikes of both fault planes are almost the same (201° and 199°, Table 1) to tangent to the equal depth lines (Fig. 1a) obtained by Nacif (2012). The 2000, 2003 ruptures are up dip and down dip respectively. We suggest that the stress change produced by the 2000 rupture in the oceanic subducted slab crust would have activated the 2003 rupture across the mantle below about 18 months later. The combined process represents, as a whole, a rupture from the subducted oceanic crust towards the upper mantle. In particular, Marot et al. (2012) propose a reactivation of a preexisting fault, 145° strike, corresponding to those generated in the Pacific Mid-ocean ridge (Contreras-Reyes et al., 2007; Kopp et al., 2004; Ranero et al., 2005).

However, the mechanisms obtained, with 201° and 199° trends, tangents to the line of 100 km depth of to the subducted Nazca plate, suggest the reactivation of an outer rise fault. This is supported by the fact that dips of the fault planes for the 2000 and 2003 earthquakes, were 56° and 65° westward dipping, respectively, considering that the plate has a slope of 27°. Therefore these values are more likely consistent with the dips of normal faults originated in the outer rise at these latitudes (Ranero and Sallares, 2004; Ranero et al., 2003, 2005).

6. Conclusions

The hypocenters of the 2000 and 2003 intermediate depth earthquakes, both located near the oceanic Moho, are found close to each other, being the ruptures up dip and down dip respectively. The spatial location of the hypocenters, their respective aftershock distributions, and the associated Coulomb stress changes, show that the slip on the west-dipping fault plane of the 2000 event increased the normal stress on the west-dipping fault plane of the 2003 event, with a variation range for this earthquake from ~1 bar near its hypocenter to ~0.1 bar in the deeper part of the plane. The 2003 rupture occurred 18 months after the occurrence of the 2000 earthquake. The combined process of both earthquakes describes a normal rupture mechanism, which cuts throughout the crust and into the mantle reaching ~40 km depth below the Moho.

Fault planes of the 2000 and 2003 rupture processes, striking 201° and 199° and dipping 29° and 38° respectively, describe a compound normal fault whose location and geometry suggest an origin in the outer ridge.

The parameters obtained, such as velocity and areas rupture, time function and isotropic-CLVD components, shed light on the dynamics of the ruptures at 120 km depth, where seismicity vanishes.

Acknowledgments

The facilities of the IRIS Data Management System, and specifically the IRIS Data Management Center, were used for access to waveform, metadata or products required in this study. Our research was founded by PICTO N°254 Riesgo Sísmico, 2011–2014, PICT-2011-1079 and UNSJ-CICITCA Proyect. Res.022/13-CS.

References

Aki, K., Richards, P.G., 1980. Quantitative Seismology. Freeman and Co., New York.
Anderson, M., Alvarado, P., Zandt, G., Beck, S., 2007. Geometry and brittle deformation of the subducting Nazca Plate, Central Chile and Argentina. Geophys. J. Int. 171, 419–434.
Barazangi, M., Isacks, B.I., 1976. Spatial distribution of earthquakes and subduction of the Nazca Plate beneath South America. Geology 4, 686–692.
Cahill, T., Isacks, B.L., 1992. Seismicity and shape of the subducted Nazca plate. J. Geophys. Res. 97, 17503–17529.
Contreras-Reyes, E., Osses, A., 2010. Lithospheric flexure modelling seaward of the Chile trench: implications for oceanic plate weakening in the trench outer rise region. Geophys. J. Int. 182 (1), 97–112.
Contreras-Reyes, E., Grevemeyer, I., Flueh, E.R., Scherwath, M., Heesemann, M., 2007. Alteration of the subducting oceanic lithosphere at the southern central Chile trench-outer rise. Geochem. Geophys. Geosystems 8 (7), 1525–2027.
Faccenda, M., Gerya, T.V., Burlini, L., 2009. Deep slab hydration induced by bending-related variations in tectonic pressure. Nat. Geosci. 2, 790–793.
Fisher, D.M., 1996. Fabrics and veins in the forearc: a record of cyclic fluid flow at depths of <15 km. In: Bebout, E., et al. (Eds.), Subduction Top to Bottom, Geophys. Monogr. Ser., vol. 96. AGU, Washington, D. C, pp. 75–89.
Frolich, C., 2006. Deep Earthquakes. Cambridge University Press, Cambridge, U. K., 574 p.
Grevemeyer, I., Kaul, N., Diaz-Naveas, J.L., Villinger, H.W., Ranero, C.R., Reichert, C., 2005. Heat flow and bending-related faulting at subduction trenches: case studies of Nicaragua and Central Chile. Earth Planet. Sci. Lett. 236 (1–2), 238–248.
Hartzell, S.H., Heaton, T.H., 1983. Inversion of strong ground motion and teleseismic waveform data for the fault rupture history of the 1979 Imperial Valley, California, earthquake. Bull. Seismol. Soc. Am. 73, 1553–1583.
Hacker, B.R., Peacock, S.M., Abers, G.A., Holloway, S.D., 2003. Subduction factory 2. Are intermediate-depth earthquakes in subducting slabs linked to metamorphic dehydration reactions? J. Geophys. Res. 108 (b1), 2030.
Jeffreys, H., Bullen, K., 1958. Seismological Tables. Office of the British Association, Burlington House, London.
Jiao, W., Silver, P.G., Fei, Y., Prewitt, C.T., 2000. Do intermediate- and deep-focus earthquakes occur on pre-existing weak zones? An examination of the Tonga subduction zone. J. Geophys. Res. 105 (B12), 28125–28138.
Jordan, T.E., Isacks, B., Allmendinger, R., Brewer, J., Ramos, V., Ando, C., 1983. Andean tectonics related to geometry of the subducted Nazca Plate. Geol. Soc. Am. Bull. 94, 341–361.
Jung, H., Fei, Y., Silver, P., Green, H., 2009. Frictional sliding in serpentine at very high pressure. Earth Planet. Sci. Lett. 277, 273–279.
Jung, H., Green II, H.W., Dobrzinetskaya, L.F., 2004. Intermediate-depth earthquake faulting by dehydration embrittlement with negative volume change. Nature 428, 545–549.
Kawakatsu, H., 1991. Insignificant isotropic component in the moment tensor of deep earthquakes. Nature 351, 50–53.
Kawakatsu, H., 1996. Observability of isotropic component of a moment tensor. Geophys. J. Int. 126, 525–544.
Kearey, P., Klepeis, K.A., Vine, F.J., 2009. Global Tectonics, third ed. (by Kearey, P., Klepeis, K.A., Vine F.J).
Kendrick, E., Bevis, M., Smalley, R.J., Brooks, B.A., Barriga, R., Lauría, E., Souto, L.P., 2003. The Nazca-South America Euler vector and its rate of change. J. South Am. Earth Sci. 16 (2), 125–131.

Kikuchi, M., Kanamori, H., 1982. Inversion of complex body waves. Bull. Seismol. Soc. Am. 72, 491–506.
Kikuchi, M., Kanamori, H., Satake, K., 1993. Source complexity of the 1988 Armenian earthquake-evidence for a slow after-slip event. J. Geophys. Res. 98, 15797–15808.
Kikuchi, M., Kanamori, H., 1991. Inversion of complex body waves III. Bull. Seismol. Soc. Am. 81, 2335–2350.
Kikuchi, M., Kanamori, H., 2003. Note on Teleseismic Body-Wave Inversion Program. http://www.eri.u-tokyo.ac.jp/ETAL/KIKUCHI/manual.pdf.
Kirby, S., Engdalh, E.R., Denlinger, R., 1996. Intermediate-depth intraslab earthquake and arc volcanism as physical expressions of crustal and uppermost mantle metamorphism in subducting slabs. In: En Bebout, G.E., School, D.W., Kirby, S.H., Platt, J.P. (Eds.), Subduction Top to Bottom, Geophysical Monograph, vol. 96. American Geophysical Union, pp. 195–214.
Kopp, H., Flueh, R., Papenberg, C., Klaeschen, D., 2004. Seismic investigations of the O'Higgins Seamount Group and Juan Fernandez Ridge: aseismic ridge emplacement and lithosphere hydration. Tectonics 23 (2), TC2009. http://dx.doi.org/10.1029/2003tc001590.
Kubas, A., Sipkin, S.A., 1987. Non-double-couple earthquake mechanisms in the nazca plate subduction. Geophys. Res. Lett. 14 (4), 339–342.
Lin, J., Stein, R.S., 2004. Stress triggering in thrust and subduction earthquakes, and stress interaction between the southern San Andreas and nearby thrust and strike-slip faults. J. Geophys. Res. 109, B02303.
Marot, M., Monfret, T., Pardo, M., Ranalli, G., Nolet, G., 2012. An intermediate-depth tensional earthquake (M_W 5.7) and its aftershocks within the Nazca slab, central Chile: a reactivated outer rise fault? Earth Planet. Sci. Lett. 327–328, 9–16.
Masters, T.G., Shearer, P.M., Ahrens, T.J., 1995. Seismic models of the Earth: elastic and anelastic. American Geophysical Union Bulletin, Polar Proj. OP-O3A4. In: Global Earth Physics: a Handbook of Physical Constants, vol. 1, no. 4. American Geophysical Union, Washington, pp. 88–103.
Meade, C., Jeanloz, R., 1991. Deep focus earthquakes and recycling of water into the Earth's mantle. Science 252, 68–72.
Nacif, S.V., 2012. Sismotectónica de la placa de Nazca entre 33°S y 35°S por debajo de la zona sismogénica de interplacas y anisotropía sísmica en la corteza y manto superior de la placa suprayacente. Ph.D. thesis. Universidad Nacional de San Juan, 217p.
Ranero, C.R., Morgan, J.P., McIntosh, K., Reichert, C., 2003. Bending-related faulting and mantle serpentinization at the Middle America trench. Nature 425, 367–373.
Ranero, C.R., Villasenor, A., Morgan, J.P., Weinrebe, W., 2005. Relationship between bend-faulting at trenches and intermediate-depth seismicity. Geochem. Geophys. Geosystems 6 (12), Q12002.
Ranero, C.R., Sallares, V., 2004. Geophysical evidence for hydration of the crust and mantle of the Nazca plate during bending at the north Chile trench. Geology 32 (7), 549–552.
Scholz, C.H., 1994. A reappraisal of large earthquake scaling. Bull. Seismol. Soc. Am. 84 (1), 215–218.
Spagnotto, S.L., 2013. Sismicidad entre 34.5-36.5°S y 67°-71°O posterior al sismo de Maule, M_w=8.8, 27/02/2010 y distribuciones de deslizamientos en placa de Nazca para sismos de profundidades mayores a 100 km en secciones plana y normal entre 31-34°S (Ph.D. thesis). In: Universidad Nacional de San Juan, 259p.
Toda, S., Stein, R., Richards-Dinger, K., Bozkurt, S., 2005. Forecasting the evolution of seismicity in southern California: animations built on earthquake stress transfer. J. Geophys. Res. 110 (B5), B05S16.
Triep, E.G., Sykes, L.R., 1997. Frequency of occurrence of moderate to great earthquakes in intracontinental regions: implications for changes in stress, earthquake prediction, and hazards assessments. J. Geophys. Res. B Solid Earth 102 (B5), 9923–9948.
Warren, L.M., Langstaa, M.A., Silver, P.G., 2008. Fault-plane orientations of intermediate-depth earthquakes in the Middle America trench. J. Geophys. Res. 113, B01304.
Wells, D.L., Coppersmith, K.J., 1994. New empirical relationships among magnitude, rupture length, rupture width, rupture area, and surface displacement. Bull. Seismol. Soc. Am. 84 (4), 974–1002.
Xia, K., Rosakis, A.J., Kanamori, H., 2004. Laboratory earthquakes: the sub-Rayleigh-to-supershear rupture transition. Science 303 (5665), 1859–1861.